Curing of Bromobutyl Elastomer Composition Using a Xanthogen Polysulphide Accelerator for Medical Drug Delivery Device Applications

D. S. Ohbi,[1] T. S. Purewal,[1] T. Shah,[2] E. Siores[2]

[1]*Bespak plc, Milton Keynes MK12 5TS, England*
[2]*Centre for Materials Research and Innovation, University of Bolton, Bolton BL3 5AB, England*

Received 1 December 2006; accepted 12 March 2007
DOI 10.1002/app.26506
Published online 26 June 2007 in Wiley InterScience (www.interscience.wiley.com).

ABSTRACT: Bromobutyl elastomer (BIIR) can be used for sealing medical drug delivery devices due to its high resistance to permeability by moisture and gases which are known to deteriorate the performance of pharmaceutical drugs. However, its use is restricted since the traditional accelerators used for crosslinking BIIR leave reaction residues which can leach out and contaminate drugs. An accelerator based on xanthogen polysulphide (DIXP) does not leave reaction residues as it is totally consumed during crosslinking. From these considerations DIXP was used to formulate a BIIR composition for seals in medical devices. The isothermal kinetic reaction curve for BIIR showed that the crosslinking region consists of two parts. The first part had a reaction order (n) = 1 and the second stage had a lower n = 0.6–0.7. The rate constants and the activation energies for the two stages were determined. Increasing the time and temperature variables of crosslinking increased the dynamic elastic shear modulus (G') in BIIR according to the kinetic theory of vulcanization, however the moisture ingress showed an initial decrease followed by an inflection where increasing the variables caused increased moisture ingress. This increase is believed to be caused by the volatile gaseous byproducts produced in the crosslinking reaction of DIXP which change the microstructure of BIIR. The crosslinking conditions for minimizing moisture ingress in BIIR and achieving a high G' were identified. © 2007 Wiley Periodicals, Inc. J Appl Polym Sci 106: 526–533, 2007

Key words: elastomer; drug delivery; crosslinking; injection molding

INTRODUCTION

Elastomeric compositions are used as seals in medical drug delivery devices. They are specifically formulated for use in these applications taking into account their toxicity, safety, and reliability of performance throughout the life of the product. Guidelines are provided by bodies such as the United States Food and Drug Administration[1] (FDA) and ISO 10,993-1 on the assessment of compounded elastomers for use in these applications. It is customary to add inorganic fillers and organic additives to the elastomer compositions for their processing and the development of physical properties. The organic additives are low molecular species such as processing aids based on fatty acids and sulfur or peroxide based crosslinking agents. The elastomer compositions are in direct contact with drug formulations and the organic additives can leach out[2] and contaminate drugs. The amounts of additives in the elastomer formulations must be optimized so that the levels of leachable by products are kept low while making sure that the curing and processing of the elastomer are not affected adversely.

BIIR is a synthetic elastomer that is a suitable material for sealing medical devices because of its inherent resistance to permeability of gases and moisture. It has low unsaturation and is predominantly isobutylene copolymerised with about 1–3 mol% isoprene to provide the reaction sites for crosslinking. The isoprene unit is brominated in the production of BIIR[3] by treating a solution of Butyl (IIR) with elemental bromine. BIIR has fewer double bonds available for crosslinking in comparison to the highly unsaturated polyisoprene elastomer. Consequently, highly efficient accelerators are required for its crosslinking. Accelerator-free crosslinking using zinc oxide can be achieved but is too slow for practical production processes. The most common accelerators used for crosslinking BIIR are based on amines and are listed in Table I.

They are highly polar materials and tend to bloom out to the surface of the elastomer. The accelerators such as thiazoles and sulfenamides liberate amines in the crosslinking reaction. The amines may also lead to other undesirable side reactions during the curing process. They can react with nitrosating agents (NO_x) to produce nitrosamines and those formed from secondary amines are stable and are

Correspondence to: D. S. Ohbi (daljit.ohbi@bespak.com).
Contract grant sponsor: Bespak plc, UK.

TABLE I
Commonly Used Accelerators for Crosslinking BIIR

Compound	Abbreviation	Type of Amine
2-Mercaptobenzthiazloe	MBT	1° primary
N-Dicyclohexylbenzthiazole–2-sulphenamide	DCBS	2° secondary
Tetramethylthiuram disulfide	TMTD	2° secondary
Zinc diethyldithiocarbamate	ZDEC	2° secondary

regarded as carcinogenic.[4] The curing reaction of an elastomer with sulfenamide accelerators can lead to the formation of MBT as a by-product.[5] The accelerators produce labile chemical entities which can migrate out into the drug mixtures and are thus potential contaminants. These contaminants and the nitrosamines are unacceptable in elastomer compositions intended for use in medical drug delivery devices; hence the choice of accelerators is severely restricted. A novel accelerator, diisopropyl xanthogen polysulphide[6] (DIXP), offers a possible solution for eliminating the undesirable vulcanization byproducts of commonly used accelerators. DIXP has is believed to be totally consumed during the vulcanization process leaving no reaction byproduct residues. A proposed reaction scheme showing the crosslinking mechanism of DIXP is shown (Fig. 1).

The reaction by-products are isopropanol and carbon disulphide and are given off as gases and diffuse out of the elastomer during the vulcanization process. Although applications of DIXP have been reported[7] in highly unsaturated natural and synthetic polyisoprene for the production of pharmaceutical stoppers, molded baby teats, etc its use for curing BIIR which has very low unsaturation is not known. The aim of this study was to determine the effect of the crosslinking conditions on the kinetics and physical properties of BIIR accelerated with DIXP. The resistance to

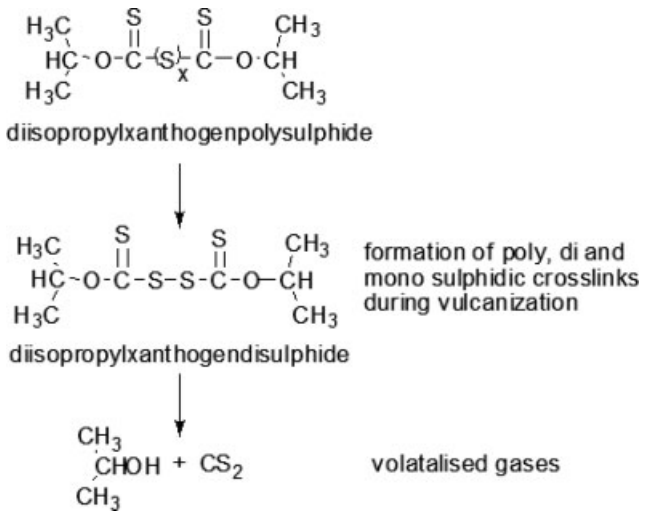

Figure 1 Crosslinking mechanism of DIXP.

moisture ingress is especially important in the pharmaceutical medical device (MDI) for dispensing asthmatic drugs as it contains propellants which are highly hygroscopic and moisture causes deleterious effects on its product performance. A high value of the dynamic elastic shear modulus G' is beneficial for the MDI seals as they undergo deformation during its actuation process. Poor elastic recovery usually results in variation of the delivered drug dose.

EXPERIMENTAL

Experimental design for molding BIIR

A quadratic response surface design (Table II) for the molding of BIIR seals for the MDI drug delivery device used in this investigation, and for the G' measurements was generated using the EChip®[8] software with time and temperature as continuous variables.

The analysis software graphically depicts the effect of variables and their interactions on the measured responses making it easy to identify processing conditions for maximizing BIIR properties. The statistically designed experiments have been successfully used by other researchers[9,10] for optimizing and developing elastomeric formulations.

Elastomer composition

The bromobutyl composition (Table III) used in this study was mixed using a K2 Intermix.

During mixing, cooling water at 30°C was circulated in the mixer body and rotors. A rotor speed of 20 revolutions per minute was maintained during the mixing process. The ingredients of the composition were commercially available rubber grade materials that meet the FDA section 177.2600 requirements for contact with food stuffs.

Characterization of bromobutyl base elastomer

The Mooney viscosity, bromine content, unsaturation level and molecular weight of the base elastomer were determined (Table IV).

TABLE II
Quadratic Response Surface Design

Trial no.	Time (min)	Temperature (°C)
1	2.0	175.0
2	2.0	165.0
3	4.5	175.0
4	7.0	175.0
5	7.0	160.0
6	2.0	160.0
7	5.0	160.0
8	4.0	160.0
9	7.0	165.0
10	7.0	170.0
11	4.0	170.0

TABLE III
Bromobutyl Composition

Material	Concentration (phr)
Bromobutyl	100
Zinc oxide	3
Stearic acid	1
Clay	80
Talc	40
Sulphur	0.5
DIXP	1.0

Determination of Mooney viscosity

The Mooney viscosity of the base elastomer was determined using a Wallace Mooney viscometer according to the ASTM D 1646-04 standard for measuring elastomer viscosity. The viscosity was measured at 125°C using large rotors of 38.10 ± 0.03 mm diameter and 5.54 ± 0.03 mm thicknesses. The sample was allowed to warm up for 1 min and after 8 min the viscosity (ML1 + 8) was measured.

Determination of bromine content

The total bromine content of the bromobutyl elastomer was analyzed by oxygen flask combustion followed by ion chromatography determination. In the combustion all the bromine present in the sample is quantitatively converted to bromide. A 1000-cm^3 oxygen flask and a stopper with a hook were used. A small platinum basket was hung from the hook and about 25 mg of the sample, wrapped in lens tissue, was placed in the basket. An absorbing solution (30% hydrogen peroxide in water) was added to the flask. The flask was thoroughly flushed with oxygen, the sample was ignited and combusted inside the flask. After the combustion the flask was shaken vigorously and allowed to stand for 45 min. The absorbing solution was then transferred to a volumetric flask and the bromide analyzed by ion chromatography determination. A standard potassium bromide solution was used as a reference.

Determination of unsaturation level

The unsaturation level of the elastomer was determined by ^{1}HNMR analysis using the Brucker AC300F NMR. Peak positions were measured against an internal reference sample tetramethylsilane (TMS).

For each sample about 10 mg was dissolved overnight in about 1 cm^3 of *d*-chloroform with 0.03% TMS internal standard. The instrument was set up to carry out 1000 scans with RF pulses of 7 μs with a delay of 6 s between each pulse. The resulting spectra were processed to show the specific peaks related to brominated (position 4.32 ppm) and CH= unsaturated groups (positions 5.39 and 5.02 ppm) and those related to the isobutyl polymer backbone (positions 1.31 and 1.11 ppm). Peak areas were measured using the instrument software and the amount of unsaturated groups estimated relative to those of the backbone. The elastomer unsaturation level was recalculated on a mole % basis.

Determination of BIIR molecular weight

Molecular weight of BIIR base elastomer was determined by GPC analysis. The sample was dissolved in tetrahydrofuran (10 mL solvent to 20 mg sample) and left overnight to ensure full dissolution. The BIIR solution was then diluted with an equal volume of solvent and filtered through 0.2 μm polyamide membrane and transferred to glass auto sampler vials for analysis. The following chromatic conditions were used:

Columns: PLgel guard plus 2 × mixed bed-B, 30 cm, 10 μm.
Solvent: Terahydrofuran with antioxidant.
Flow-rate: 1.0 mL min^{-1} (nominal)
Temperature: 30°C (nominal).
Detector: Refractive index (with differential pressure and light scattering).

The GPC was calibrated with polystyrene standards and the molecular weights are expressed as polystyrene equivalent molecular weights.

Determination of kinetics of crosslinking

The kinetics of the crosslinking reaction for BIIR was determined using the RPA 2000 at temperatures of 150, 160, 170, and 190°C. The BIIR sample was enclosed in a heated die with the lower die oscillating at 1.667 Hz at an arc of 0.5°. The torque required to maintain the die oscillations increases with time due to the increase in crosslink density of the sample.

The reaction rate constant (k) was determined from the isotherm using the method of Scheele.[11] The 1st order reaction kinetics is described by eq. (1).

$$\ln\left(\frac{Y_\infty - Y}{Y_\infty - Y_0}\right) = C - kt \tag{1}$$

TABLE IV
Characterisation of BIIR Base Elastomer

Mooney Viscosity (ML1 + 8)	46
Bromine content	2.01 wt %
Unsaturation	1.8 mole %
Unsaturation	2.2 wt %
M_w	523,000
M_n	172,000

If the reaction order $n \neq 1$, reaction rate is described by eq. (2) and when n is < 1 values are substituted in eq. (2) and if the plot is a straight line, order of the reaction is obtained.

$$\frac{1}{1-n}\left(\frac{Y_\infty - Y}{Y_\infty - Y_0}\right)^{1-n} = C' - kt \quad (2)$$

Y_0 = initial torque (uncrosslinked sample), Y torque at time t, Y_∞ maximum torque at $t = \infty$, and C and C' are constants.

The rate constant k was obtained from the negative slope $= -k$.

The activation energy E was calculated using the Arrhenius eq. (3).

$$\ln k \propto -\frac{E}{RT} \quad (3)$$

Determination of Shear modulus (G')

The RPA 2000 has been used[12] both for curing elastomers and for determination of dynamic properties such as G' and loss tangent δ. The BIIR compositions were cured using the RPA 2000 according to the times and temperatures (Table II). Compressed air was used to cool the crosslinked BIIR sample contained in the dies to 50°C and which was then allowed to equilibrate at this temperature for 10 min. The G' of BIIR was obtained at 50°C with strain fixed at 1.95% and frequency 0.1 Hz.

Injection molding of BIIR seals for MDI device

BIIR seals for the MDI device were molded using the Engel E330/80HL rubber injection molding machine. The injection molding settings were; injection pressure 159 bar, injection speed 8 mm s^{-1}, and screw back pressure 160–60 bar and nozzle orifice diameter 35 mm. The molding time and temperature conditions are given in Table II. After molding the seals were extracted with ethanol for 48 h at 60°C to remove ethanol soluble residues. The extraction procedure was carried out to minimize carryover of extraneous impurities into the MDI's.

MDI test units

The BIIR seals were used to construct MDI valves having a metering chamber size of 50 μL which were crimped onto 19 mL aluminum cans. The basic design of the MDI unit with the elastomer seals (two seats and gasket) is shown (Fig. 2).

Determination of moisture ingress into the MDI

The MDIs were filled with a placebo mixture of 10% ethanol and 90% 1, 1, 1, 2-tetrafluoroethane (HFA 134a) and allowed to equilibrate in a valve down position at room temperature for 1 week. The moisture (water) ingress into the MDI occurs predominantly through the amorphous BIIR seals and was determined using the Metrohm 831 Coulometric Karl Fischer titrator. The titrator was calibrated using certified Hydranat® 1.0 standard solution which contains 1.00 ± 0.003 ppm water. The MDI test unit was connected to the titrator using an adaptor and fired five times and the water content determined. The weight determinations were made using an analytical balance with resolution of 0.01 mg. This procedure was repeated three times to determine the average water content. After moisture content measurements, the MDIs were stored in a valve down position in an environmental chamber maintained at 40°C and 75% relative humidity (RH). At defined time points, the test samples were removed from the chamber and allowed to equilibrate at 20°C and 33% (RH) for 4 h before taking the final readings.

RESULTS AND DISCUSSION

Reaction kinetics

The crosslinking kinetic curve (Fig. 3) for BIIR using DIXP obtained at 170°C, exhibits three regions, induction, crosslinking and the post crosslinking.

These regions are typically seen in the crosslinking of elastomers. The chemical and kinetic changes associated with these stages have been reported[13–15] by various researchers. The crosslinking region exhibits two parts and the kinetic reaction order and activation energy of each part is shown (Table V).

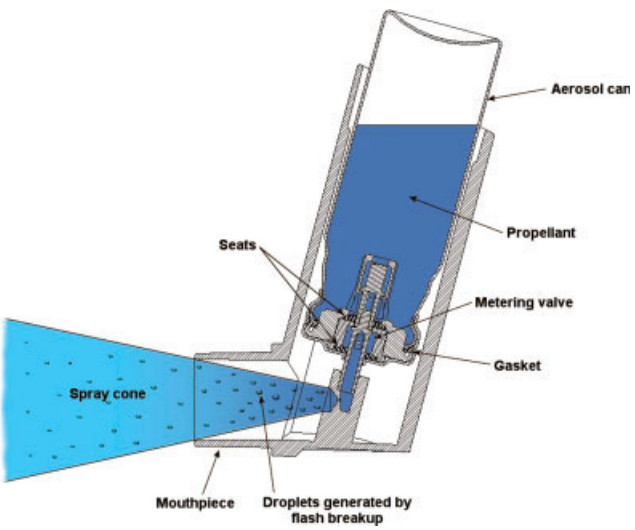

Figure 2 Design of MDI showing the position of the elastomer seals. [Color figure can be viewed in the online issue, which is available at www.interscience.wiley.com.]

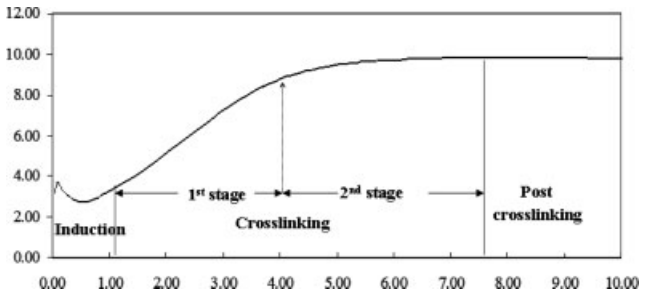

Figure 3 Kinetic curve for BIIR at 170°C. Vertical axis shows torque Y in dNm and horizontal time t in minutes.

The linear part exhibits first order kinetics according to eq. (1) with the formation of poly, di, and monosulphidic crosslinks according to the proposed reaction mechanism of DIXP (Fig. 1). The second curved part had a reaction order n = 0.6–0.7 and by substituting these values in eq. (2) produced straight lines (Fig. 4) verifying the reaction order. In this part changes involving shortening of some of the polysulphidic crosslinks[16] for example to di and monosulfur crosslinks could be occurring.

E for both parts was calculated using eq. (3). The first part has a faster k and a higher E than the latter. Wang et al.[17] also found similar two part kinetic behavior for a natural rubber composition accelerated with MBT. The activation energy for BIIR using DIXP lies in the range 71.8–123.3 kJ mol^{-1} determined for Butyl compositions accelerated with MBT and thiourea by Rodgers et al.[18] The activity of DIXP in BIIR is thus similar to these commonly used accelerators.

EChip analysis

Results for moisture ingress and G' from the 11 different trials and five replicates are given in Table VI.

The data was analyzed by EChip® and curve fit response surface models were produced for both responses.

Shear modulus G'

The EChip® software was used in the regression analysis of the time and temperature effect on G' to determine the best fit polynomial eq. (4).

$$\begin{aligned} G' = {} & 1208.88 + 69.9521(\text{time} - 4.5) \\ & + 17.752(\text{temperature} - 167.5) \\ & - 3.21986(\text{time} - 4.5) \times (\text{temperature} - 167.5) \\ & - 9.14646(\text{time} - 4.5)^2 \\ & - 0.280752(\text{temperature} - 167.5)^2 \end{aligned} \quad (4)$$

The G' response curves are shown in Figure 5. The significance of the terms in the best fit equation is rated by EChip®. The time, temperature, time and temperature interaction (time × temperature), and the time^2 terms in eq. (4) have highly significant effects on G'.

Increasing the time increases G', as the number of crosslinks formed in the BIIR network increase. At a fixed time, increasing temperature from 160 to 175°C increases G' due to the faster formation of crosslinks as shown by the rate constants k (Table V). The highly significant time^2 term in eq. (4) predicts a cur-

TABLE V
Kinetic Summary for the Crosslinking of BIIR

	Crosslinking temperature				
	150°C	160°C	170°C	180°C	190°C
1st part	n = 1	n = 1	n = 1	n = 1	n = 1
k	0.1009	0.2274	0.5709	0.9617	2.0978
C	0.4359	0.4717	0.4697	0.6454	1.0688
RSQ	0.9937	0.9916	0.9919	0.9960	0.9995
2nd part	n = 0.61	n = 0.65	n = 0.7	n = 0.6	n = 0.6
K'	0.0612	0.0951	0.1812	0.3463	0.7688
C′	1.7592	1.4692	1.5097	1.3394	1.5738
RSQ	0.9954	0.9970	0.9955	0.9972	0.9944

	Activation energy	
	E (kJ mol^{-1})	RSQ
1st part (n = 1)	122.6	0.9955
2nd part (n = 0.6–0.7)	103.3	0.9845

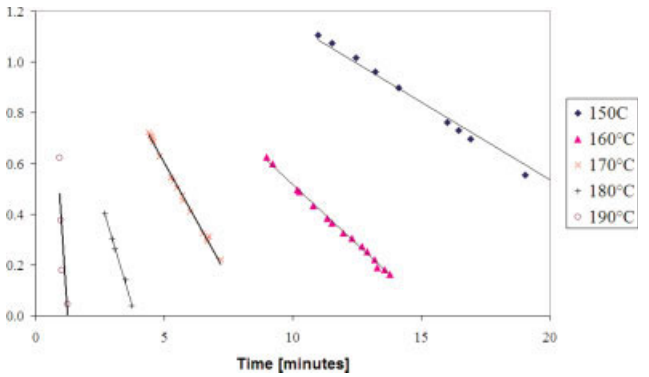

Figure 4 Determination of the rate second stage k. Vertical axis shows $\frac{1}{1-n}\left(\frac{Y_\infty - Y}{Y_\infty - Y_0}\right)^{1-n}$. [Color figure can be viewed in the online issue, which is available at www.interscience.wiley.com.]

vature in the response curve and increasing crosslinking time beyond 7 min time would lower G'. This is due to a phenomenon known as reversion[16,19] where competing crosslinking desulpuration reactions occur and the physical properties like G' are lowered through destruction and or the formation of ineffective crosslinks. The predicted maximum G' for BIIR crosslinked using DIXP is indicated by the arrow in the response surface (Fig. 5) is at 7 min at 175°C.

Resistance to moisture permeability

The moisture ingress response surface curve is described by the polynomial eq. (5).

TABLE VI
Moisture Results After 3 Months Storage at 40°C/75% Relative Humidity. G′ Results Obtained Using RPA2000 at Strain 1.95% and Frequency 0.1 Hz

	Responses	
Trial no.	Moisture (mg) (ppm)	G′ (kPa)
1	672	1159.7
2	715	872.33
3	781	1350.4
4	999	1365.8
5	685	1251.9
6	745	793.25
7	641	1081.3
8	775	970.9
9	805	1330.9
10	844	1314.1
11	617	1250
3R	595	1332.2
5R	679	1237.6
6R	729	794.16
10R	848	1360.3
1R	671	1134.4

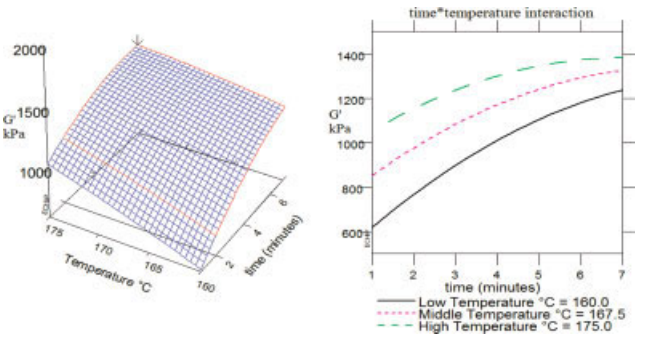

Figure 5 Time temperature response curves for G'. [Color figure can be viewed in the online issue, which is available at www.interscience.wiley.com.]

$$\begin{aligned}\text{Moisture} = {} & 656.17 + 25.2886(\text{time} - 4.5) \\ & + 4.4476(\text{temperature} - 167.5) \\ & + 4.9539(\text{time} - 4.5) \times (\text{temperature} - 167.5) \\ & + 13.8971(\text{time} - 4.5)^2 \\ & + 0.5312(\text{temperature} - 167.5)^2 \end{aligned} \quad (6)$$

The moisture ingress response curves are shown in Figure 6.

The terms time, time^2, and (time × temperature) in eq. (5) have highly significant effects on the moisture ingress. At all crosslinking temperatures, moisture ingress shows a concave response with respect to the time axis. The initial decrease in moisture ingress with time is due to the build up of crosslink density in BIIR and the process is quicker with higher temperature due to the temperature effect on k (Table V). The increase in moisture ingress shown by the curvature (time^2 effect) is higher at higher temperatures.

This effect appears to be related to the chemical crosslinking reaction of DIXP (Fig. 1). DIXP is totally consumed in this reaction forming the poly, di, and mono sulfidic crosslinks and gaseous byproducts

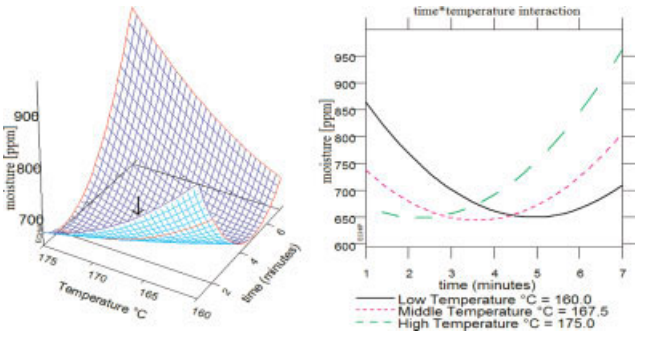

Figure 6 Time–temperature response curves for the moisture ingress. Measurements at 3 months and at 40°C/75% RH. [Color figure can be viewed in the online issue, which is available at www.interscience.wiley.com.]

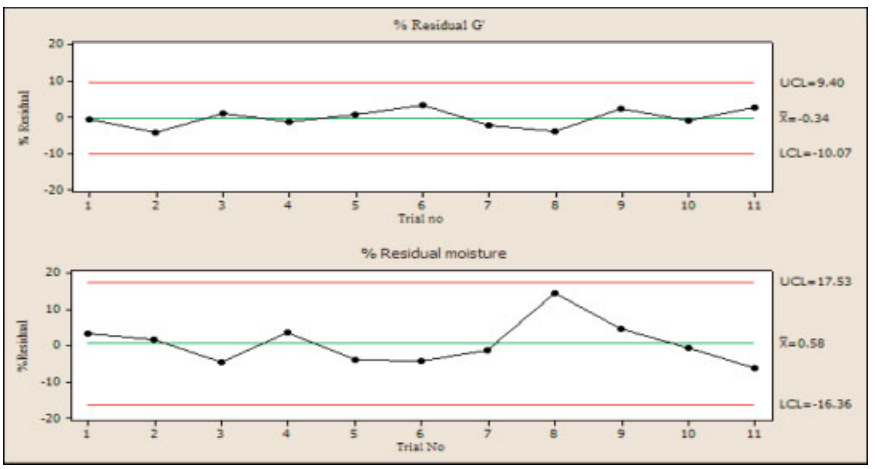

Figure 7 Percentage residuals for experimental trials. [Color figure can be viewed in the online issue, which is available at www.interscience.wiley.com.]

which could affect the microstructure of BIIR causing the increase in moisture ingress. This aspect is being investigated and will form part of a future publication. The point of minimum moisture ingress predicted by EChip® is shown by the arrow (Fig. 6) is at 4 min and 170°C.

Comparison between predicted and experimental properties

The percentage residuals (difference between observed and predicted values) for the moisture and G' responses are plotted in Figure 7.

The residuals for G' are small indicating a good fit to its response surface model. For the moisture response, trial 8 shows a high residual (14.5%) and adds a degree of uncertainty to the model predictions. While the predictability of the moisture response is not as good as G', the model describing it is quite adequate as the range of residuals is within the 3-sigma limits. These limits were selected as they are used routinely to indicate acceptable product quality in industrial processes.

Optimization of curing conditions for BIIR

The optimum time and molding temperature values (Table VII) for maximizing the moisture resistance and G' of BIIR elastomer were determined by EChip® analysis in which an equal weighting was given to both responses.

TABLE VII
Optimized Moulding Conditions for BIIR

Response	Cure time	Mean	Low limit	High limit
Moisture	4 min at 170°C	655 ppm	496 ppm	815 ppm
G'	4 min at 170°C	1218 kPa	1140 kPa	1296 kPa

CONCLUSIONS

The effect of a xanthogen polysulphide based accelerator, DIXP on the curing behavior of bromobutyl elastomer was studied using experimental design and statistical analysis methods. The continuous time and temperature variables have significant influence on the kinetics and the physical properties of BIIR. The shear modulus G' increases with time and with temperature (160 to 175°C) however increasing time beyond 7 min could lead to reversion and the lowering of G'. The resistance to moisture ingress shows a concave curvature to the time axis and increasing time beyond the minimum deteriorates this property, and higher crosslinking temperatures lead to higher moisture ingress. This effect is attributed to changes in the microstructure of BIIR probably caused by the gaseous byproducts of the crosslinking reaction of DIXP.

The elastomer moisture ingress and shear modulus are important characteristics for sealing medical drug delivery devices as they influence the life of the product. The use of DIXP for crosslinking BIIR does not create reaction byproducts which would leach out and contaminate drugs. The optimum vulcanization condition for maximizing the BIIR resistance to moisture ingress and obtaining a high shear modulus was found to be 4 min at 170°C.

The crosslinking kinetics of BIIR accelerated with DIXP, shows two stage behavior; initially the reaction is 1st order, and in the second part is of lower order with $n = 0.6–0.7$. The activation energy measured for the two parts are 122.6 and 103.3 kJ mol^{-1}, respectively. The activity of DIXP in BIIR was found

to be comparable to MBTS/thiourea accelerators used in Butyl rubber.

The authors thank R. J. Warby, R and D Manager, Respiratory Department, for his invaluable support and discussions in this project.

References

1. Pharmacopeia, United States. In USP 29-NF 24; Webcom Limited: Rockville, 2006; Chapter 87.
2. McMillin, C. R. Rubber Chem Technol 1994, 67, 417.
3. Meissner, B.; Schatz, M.; Brajko, V. In Elastomers and Rubber Compounding Materials; Franta, I., Ed.; Elsevier: Oxford, 1989; Chapter 4.
4. Layer, R. W.; Chasar, D. W. Rubber Chem Technol 1994, 67, 299.
5. Coran, A. Y. In Science and Technology of Rubbers; Mark, J. E.; Erman, B.; Eirich, F. R., Eds.; Academic Press: Sav Diego, 1994; Chapter 7.
6. Chakraborty, K. B.; Couchman, R. In the North European International Conference-IRC 2005; Media Business Press Maastricht, The Netherlands, 2005; p 8.
7. Couchman, R.; Chakraborty, K. B. Automobile Elastomers Conference, Dearborn, Michigan, June 15–16, 2004; Paper 14.
8. Wheeler, B.; Betch, R.; Donnelly, T. ECHIP Design of Experiments; ECHIP: Hockessin, 2005.
9. Thomas, N. L.; Gilbert, M.; Haong, T. Plast Rubber Compos 2006, 35, 112.
10. Thorn, A. D.; Robinson, R. A. In Rubber Products Manufacturing Technology; Bhowmick, A. K.; Hall, M. M.; Benarey, H. A., Eds.; Marcel Dekker: New York, 1994; Chapter 1.
11. Sheele, L. KatuschGummiKunst 1965, 43, 138.
12. Chattaraj, P. P.; Mukhopadhyay, R. Rubber Chem Technol 1997, 70, 91.
13. Ding, A.; Leonov, A. I.; Coran, A. Y. Rubber Chem Technol 1996, 69, 81.
14. Isayev, A. I.; Sujan, B. Elastomers Plast 2006, 38, 291.
15. Bhowmick, A. K.; De, S. K. Rubber Chem Technol 1980, 53, 1015.
16. Aprem, A. S.; Joseph, K.; Thomas, K. Rubber Chem Technol 2005, 78, 458.
17. Wang, P.-Y.; Quinn, H.-L.; Yu, H.-P. J Appl Polm Sci 2006, 101, 280.
18. Rodgers, B.; Solis, S.; Tambe, N.; Sharma, B. B.; Waddel, H. Rubber World 2006, 233, 29.
19. Morrison, N. J.; Porter, M. Rubber Chem Technol 1984, 57, 63.